Hindawi
International Journal of Polymer Science
Volume 2020, Article ID 8017035, 13 pages
https://doi.org/10.1155/2020/8017035

Research Article

Effect of Temperature on Drug Release: Production of 5-FU-Encapsulated Hydroxyapatite-Gelatin Polymer Composites via Spray Drying and Analysis of In Vitro Kinetics

Nalan Erdöl Aydin

Chemical Engineering Department, Chemical-Metallurgical Faculty, Istanbul Technical University, 34469, Maslak, Istanbul, Turkey

Correspondence should be addressed to Nalan Erdöl Aydin; erdol@itu.edu.tr

Received 31 October 2019; Revised 23 January 2020; Accepted 27 February 2020; Published 23 March 2020

Academic Editor: Huining Xiao

In this study, 5-fluorouracil- (5-FU-) loaded hydroxyapatite-gelatin (HAp-GEL) polymer composites were produced in the presence of a simulated body fluid (SBF) to investigate the effects of temperature and cross-linking agents on drug release. The composites were produced by wet precipitation at pH 7.4 and temperature 37°C using glutaraldehyde (GA) as the cross-linker. The effects of different amounts of glutaraldehyde on drug release profiles were studied. Encapsulation (drug loading) was performed with 5-FU using a spray drier, and the drug release of 5-FU from the HAp-GEL composites was determined at temperatures of 32°C, 37°C, and 42°C. Different mathematical models were used to obtain the release mechanism of the drug. The morphologies and structures of the composites were analyzed by X-ray diffraction, thermal gravimetric analysis, Fourier transform infrared spectroscopy, and scanning electron microscopy. The results demonstrated that for the HAp-GEL composites, the initial burst decreased with increasing GA content at all three studied temperatures. Further, three kinetic models were investigated, and it was determined that all the composites best fit the Higuchi model. It was concluded that the drug-loaded HAp-GEL composites have the potential to be used in drug delivery applications.

1. Introduction

Hydroxyapatite (HAp,$Ca_{10}(PO_4)_6(OH)_2$) is a biomaterial found in bone and teeth, which has an apatite-like structure [1, 2]. Because of its excellent chemical stability, biocompatibility, bioactivity, nontoxicity, and osteoconductivity, HAp has been used for the production of synthetic bone materials and bone and teeth implants and in drug delivery applications [2–8]. Studies have described diverse methods for synthesizing HAp, such as hydrothermal [9, 10], sol-gel [11], microemulsion [12], precipitation [13], solid-state reaction [14], and microwave [15] methods. However, the highly brittle and stiff structure of HAp limits its usage in clinical applications [16, 17]. These mechanical disadvantages can be overcome by adding a polymer. Thus, many studies have utilized natural polymers, such as collagen, chitosan, gelatin, alginate, and starch-based materials to modify HAp and produce high-quality HAp-bioceramics [8, 18–23]. Biopolymers have excellent biocompatibility, more biodegradability, and adequate osteoconductivity [17, 24]. Among these polymers, gelatin (GEL) is widely used in drug release systems alone or in composite form [25]. In addition, gelatin has efficient swelling-releasing characteristics and does not produce antigens [16]. However, its drawbacks are high water solubility and low mechanical properties. To prevent its solubility in cell culture, cross-linking is applied [24]. Cross-linking of GEL increases its mechanical and thermal strength. For the chemical cross-linking of gelatin, cross-linking agents, such as glutaraldehyde and formaldehyde, can be applied. Glutaraldehyde (GA) is the most commonly applied agent because of its low cost and high stabilization efficiency [26–29]. Bera et al. produced HAp-GEL nanocomposites in different ratios and investigated their biocompatibility. It has been concluded that the use of high GEL concentrations covers HAp crystals more intensively and prevents their growth of the crystals [30]. HAp-GEL composite microspheres have been prepared using a wet-chemical method. The porosity of HAp-GEL provides a high ratio of surface area to void

regions, making it suitable for use as a drug carrier [17, 31]. A composite immunoisolation membrane combining GA-cross-linked GEL and HAp was designed for enclosing microencapsulated insulinoma cells [32]. Ghorbani et al. synthesized HAp-GEL scaffolds, containing dexamethasone-loaded poly(lactide-co-glycolide) microspheres by a freeze casting technique. The results showed that the HAp-GEL scaffolds have the necessary features to regenerate defects, especially at low freezing gradients and high amounts of HAp, and can serve as a basis for future cellular studies to evaluate the effect of these drug-release constructs on cellular differentiation and expression of osteogenic markers [33]. Ture [34] developed a composite wound dressing material consisting of alginate and gelatin with HAp to replace existing wound dressing materials. Examination of the swelling behaviors of the films indicated that the water retention capacities of the material decreased as the amounts of alginate and HAp in the films increased.

Because of the undesired side effects and high costs of treatments systematically carried out with antibiotics, studies regarding the controlled drug release conducted with drug-loaded composite materials have gained importance. In the controlled drug release systems, the release profile begins with small changes followed by an initial burst release, after which the release continues at almost a constant rate [35]. In the studies on drug release conducted with bioactive substances, drug release has been observed to be associated with the porosity and permeability of the substance [36]. The porous structure of HAp is similar to that of a bone's inorganic phase because of which HAp has become a preferred substance for drug loading. Studies on HAp-heparin/-GEL trilayer composites showed microspheres to be more convenient for usage in the drug release systems because of their suitability for controlled drug release at long periods of time and their high drug loading efficiency [37]. Teng et al. produced HAp-GEL microspheres by the water emulsion inside oil method and concluded that the microspheres obtained ensured homogeneous drug distribution. The existence of pores increases the drug loading capacity and is convenient for use in controlled drug release [38].

Previous studies have analyzed the loading capacity of drugs such as ibuprofen and tetracycline and their release by HAp-GEL composites containing implant and nanoparticles [35, 39]. Chen-Dou et al. examined the drug release profile of HAp-GEL composites loaded with minocycline, which is a type of semisynthetic tetracycline-derived antibiotics. It was concluded that the stable and slow release observed during the study may be related to the starting of the deformation of gelatin and hydroxyapatite [40]. The drug release profiles of gentamicin- [41], insulin- [42], and vitamin D3- (VD3-) [43] loaded HAp-GEL microspheres were examined, and the release mechanism suggested included the absorption of the environment liquid within the pores of the microspheres, dissolution of drug/insulin/VD3 in the liquid, and release of the liquid from the pores together with drug/-insulin/VD3. 5-FU used in this study has been widely applied in the treatment of many cancers such as colon, breast, ovary, pancreas, stomach, brain, and skin cancer [44, 45]. Encapsulation of the drug using natural and synthetic polymers with controlled 5-FU release for the purpose of maximizing the therapeutic properties and minimizing side effects has been studied. Some polymers used for drug release include chitosan [45], gelatin [46], poly(lactide-co-glycolide) [25], poly(d,l-lactide) [47], poly(methylidenemalonate 2.1.2) [48], and pectin [49] with 5-FU. In addition, researchers have also studied controlled drug release with composite substances such as 5-FU-loaded HAp/PLGA [50], gelatin/chitosan [51], alginate/pluronic F127/eudragitRS 100 [52], and magnetic nanocomposite [53]. Santos et al. produced 5-FU-loaded HAp nanoparticles using a spray drier, and it was concluded that HAp is not sufficient alone for controlled release [54]. The speed of 5-FU release was controlled by changing the amount of the cross-linking agent [46]. In studies on GEL-chitosan microspheres in which GA was used as the cross-linking agent and 5-FU as active principle, the initial burst release ratio was observed to decrease when the cross-linking agent amount was increased [46, 51]. The drug release profile of 5-FU-loaded HAp/PLGA composite microspheres was examined, and when the HAp/PLGA ratios were varied, it was observed that the initial burst release decreased with increasing HAp ratio [50].

Drug release mechanisms vary depending on many factors, such as the pore dimension of the drug carrier substance [31], bondability, drug/carrier interaction, and drug/polymer deformation speed. Therefore, the release mechanism needs to be determined before application [55]. Mathematical models can be used for the release kinetics using physical parameters, such as drug diffusion coefficient, and can also contribute to the optimization of the release process [56]. The in vitro drug release mechanism can be determined by measurements taken in phosphate buffer saline (PBS) or simulated body fluid (SBF) environments [57]. The pH of tumor tissues is lower than that of the normal tissues. pH controllable drug delivery system has become a hot topic because of the different pH in the physiological environment (~7.4) and tumor cell (~5.0–7.0). To achieve the drug release, stable drug delivery systems must be prepared first [58–62]. When acidic conditions (pH = 5) were applied, a faster release rate of the drug was observed [63]. Some tumor tissues have different temperatures compared with the host basal temperature because of an increased metabolic rate. Moreover, additional temperature differences can be induced by the external heating of the tumor region, e.g., by ultrasound treatment, magnetic field, or light-sensitive imaging techniques, such as radiology and optical imaging [64–67]. Thus, the effect of temperature on the drug release profile can be investigated at different temperatures.

In the current study, HAp-GEL composites were fabricated in the presence of SBF, and spray drying was used to obtain drug-loaded composites. 5-FU, which is widely used for the treatment of different cancer types, was selected as the drug [44]. Composites were produced by wet precipitation using GA as the cross-linking agent. To observe the effect of temperature, drug release studies were performed at temperatures of 32°C, 37°C, and 42°C in PBS at pH 4.0. Drug release profiles were evaluated according to three different kinetic models including zero order, first order, and

Table 1: Reactants used for the SBF preparation.

Reactant	Quantity
NaCl	7.996 g
$NaHCO_3$	0.350 g
KCl	0.224 g
$K_2HPO_4{\cdot}3H_2O$	0.228 g
$MgCl_2{\cdot}6H_2O$	0.305 g
1 M HCl	40 mL
$CaCl_2$	0.278 g
Na_2SO_4	0.071 g
$(CH_2OH)_3CNH_2$	6.057 g

Higuchi. The obtained composites were characterized by XRD, TGA, FTIR, and SEM.

To the best of our knowledge, the impact of the different release temperatures of HAp-GEL composites loaded with 5-FU using a spray dryer has not been investigated thus far.

2. Materials and Methods

Experimental stages consisted of the preparation of SBF and PBS, the production of HAp-polymer composites in SBF with GA (two different ratios as 2% (*v*/*v*) and 5% (*v*/*v*)) as a cross-linking agent, the encapsulation (drug loading) of 5-FU in HAp-polymer using a spray dryer, and in vitro drug release in a PBS medium at different temperatures.

2.1. Materials. The materials used for the HAp-GEL composites preparation, including gelatin, calcium hydroxide ($Ca(OH)_2$, 96%), phosphoric acid (H_3PO_4, 85%), and GA, were purchased from Merck (Germany). The 5-FU drug was obtained from Sigma-Aldrich (Germany). The reactants used for the SBF preparation are listed in Table 1. Sodium chloride (NaCl), sodium hydrogen carbonate ($NaHCO_3$), potassium chloride (KCl), di-potassium hydrogen phosphate trihydrate ($K_2HPO_4.3H_2O$), magnesium chloride hexahydrate ($MgCl_2.6H_2O$), calcium chloride ($CaCl_2$), sodium sulfate (Na_2SO_4), and hydrochloric acid (HCl) were obtained from Merck, and tris(hydroxymethyl) aminomethane ($(CH_2OH)_3CNH_2$) was provided by Sigma-Aldrich. Potassium phosphate dibasic (K_2HPO_4) and potassium phosphate monobasic (KH_2PO_4), which were used for the PBS preparation, were obtained from Merck and Carlo Erba (Germany), respectively.

2.2. SBF and PBS Preparation. To obtain the SBF, the reactants in Table 1 were added to 750 mL deionized water in the given order and were dissolved under constant stirring at 37°C. To prevent an instant pH increase, $(CH_2OH)_3CNH_2$ was dissolved slowly. Following the addition of the reactants, 1 M HCl was used to adjust the pH to 7.4. The solution was kept at 25°C for 1 day, and afterwards, its volume was made to 1 L by adding deionized water. K_2HPO_4 (80.2 mL, 1 M) and 19.8 mL 1 M KH_2PO_4 were prepared and mixed to obtain the PBS solution. The mixture was completed to 1 L with deionized water and was adjusted to pH 4.0 with 1 M HCl solution.

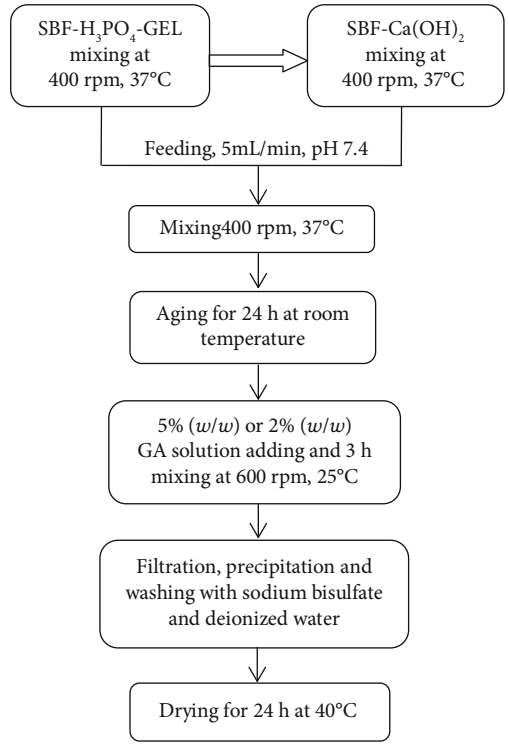

Figure 1: Flowsheet of the production of the HAp-GEL composites.

2.3. Production of HAp-Polymer Composites in an SBF Medium. Figure 1 shows the production steps of HAp-GEL polymer composites. $Ca(OH)_2$-SBF and H_3PO_4 (85%)-GEL-SBF solutions were prepared separately and were mixed using a mechanical mixer for 2 h at 37°C and 400 rpm. Then, the H_3PO_4 (85%)-GEL-SBF solution was fed to the $Ca(OH)_2$-SBF using a peristaltic pump at a feeding rate of 5 mL/min leading to the formation of HAp crystals in the solution. If necessary, the pH value of the solution was adjusted to 7.4 with the help of 1 M HCl or 1 M NaOH solutions. The obtained solution was mixed at 37°C and 400 rpm for another 2 h and was allowed to rest. After 24 h of aging for the completion of the HAp crystal growth, a GA-deionized water solution (5%/2%) (*v*/*v*) was added to the solution for cross-linking and was mixed at 600 rpm for 3 h. Then, the solution was filtered, and precipitated composites were washed with sodium bisulfate (3%) and deionized water to remove all nonreacted GA. After filtering, the precipitate was dried in an oven at 40°C for 24 h. Composites with a 1 : 1 HAp/GEL weight ratio were obtained and cross-linked with a 2% (*v*/*v*) and 5% (*v*/*v*) GA-deionized water solution.

2.4. Encapsulation (Drug Loading) Process in Spray Dryer. Seventy-five milligrams of drug was dissolved in 300 mL deionized water. This drug solution was mixed at 800 rpm for 30 min. Then, 3 g of polymer-composite sample was added, and mixing was continued. The 5-FU-loaded HAp-GEL composites were prepared using a spray dryer (Yamato ADL310) at 80°C inlet temperature of hot air, 5 mL/min inlet flow of feeding solution, and 0.1 MPa atomizer pressure.

2.5. In Vitro Drug Release in the PBS Medium. Twelve milligrams of drug-loaded HAp-GEL sample was weighed and added to tubes containing 20 mL of PBS. In vitro release studies were carried out in a shaking water bath at 200 rpm. The composites were suspended in the PBS medium at 32°C, 37°C, and 42°C and pH 4.0. At predetermined time intervals (5, 10, 15, 30, and 45 min and 1, 2, 3, and 5 h), samples were taken from the solution and were centrifuged for several minutes. Each time after removing the samples, fresh PBS was added to the solution. The 5-FU concentration in the release medium was evaluated using a UV-vis spectrophotometer (Jenway 6305) at a wavelength of 266 nm in triplicate. The released cumulative drug amounts were calculated using the attained absorbance values, and release profiles were formed according to zero order, first order, and Higuchi kinetic models.

2.6. Characterization of the Composites. The crystallinities of the composites were analyzed by XRD (Bruker D8 Advance). The comparative TGA (TA SDT Q600) patterns consisted of weight loss (%) versus temperature (°C) curves of the HAp-GEL (1 : 1) composites. By FTIR (Shimadzu), characteristic functional groups were identified in the wavenumber range of 800-4000. The morphologies of the spray-dried HAp-GEL composites with different amounts of GA were observed by SEM (Quanta FEG 250).

2.7. Release Kinetics of 5-FU. A suitable kinetic model to describe the release process is helpful for gaining insight into the release characteristics. The mathematical fitting models given by the linear equations (1)–(3) were applied to confirm and explain the in vitro release of the model drug (5-FU) from HAp-GEL in the PBS. The models used are listed below:

(i) Zero order

$$M_t = M_0 + K_0 t \tag{1}$$

(ii) First order

$$\log C = \log C_0 - \frac{Kt}{2.303} \tag{2}$$

(iii) Higuchi model

$$\text{ft} = Q = K_H \times t^{1/2}, \tag{3}$$

where Q and M_t are the cumulative amounts of drug released at time t, C_0 is the initial concentration of the drug, and K_0, K, and K_H are constants as indicated by equations (1), (2), and (3) of the concerned model corresponding to the structural and geometrical characters of the dosage form. The zero-order model describes a system where the drug release rate is independent of its concentration. The first-order model is used to describe the absorption and elimination of some drugs, although it is difficult to understand the mechanism on a theoretical basis. Finally, the Higuchi model describes the drug release as a diffusion process based on Fick's law and is a square-root-of-time-dependent mechanism. This model is often applicable to different geometrics and porous systems [68–72].

3. Results and Discussions

3.1. XRD Analysis of HAp-GEL Composites. The XRD patterns of the composites cross-linked with different amounts of GA (2% and 5% GA solutions) are presented in Figure 2 and indicate the existence of HAp in the composites. For both samples shown in Figure 2, characteristic HAp peaks were observed, confirming the formation of HAp crystals. Calcium phosphate phases other than HAp were not detected. In the 2% GA HAp-GEL composite, the presence of HAp was confirmed by the characteristic peaks at 2 Theta (θ) values of 25.94°, 31.79°, 39.61°, 46.66°, 49.47°, and 53.22°. In the 5% GA HAp-GEL composite, HAp peaks were detected at 2 Theta (θ) values of 26.01°, 31.85°, 39.81°, 46.67°, 49.57°, and 53.33°. Composites with different GA amounts had similar intensities and diffraction angles in their XRD patterns, which proves that the GA amount did not have a distinctive effect on the crystallinity of HAp-GEL. No other impurities (like CaO or TCP) were observed. These results are compatible with the results of previous studies [73, 74]. Moreover, calcium ions and $(\text{R-COO})^-$ groups of GEL interact with each other by covalent bonds, which leads to the formation of the Ca-GEL complex. This complex stopped the reaction of Ca-P ions, thus inhibiting hydroxyapatite formation [75–77]. Additionally, 210 and 110 peaks were bonded together, which could be attributed to the interaction of gelatin and hydroxyapatite [41].

3.2. TGA Analysis of the HAp-GEL Composites. The thermogravimetric analysis of the composite shows a gradual degradation of the organic content. The comparative TGA of HAp-GEL (1 : 1) composites, pure HAp, and pure GEL is given in Figure 3, which shows the weight loss (%) vs. temperature (°C) curves for the HAp-GEL-2% GA and HAp-GEL-5% GA. The GEL phase in the HAp-GEL composites is gradually degraded. The first step of the curve is related to adsorbed water molecules, which disappear at temperatures above 90°C [78]. Around 160°C, the GEL molecules gradually start to degrade and continue to burn steadily till about 300°C, and then the rate of burning gradually decreases. Finally, the pyrolysis of the remaining organic content commences at about 520-530°C. When the temperature reaches 550°C, only the inorganic HAp phase in the composites remained undegraded. This gradual degradation and pyrolysis profiles of the composites give an insight into both intramolecular and intermolecular interactions of GEL in the composites. The initial degradation probably starts with the cleaving of intramolecular bonds of GEL (a denatured protein), resulting in the loss of secondary structures commencing at about 160°C [30].

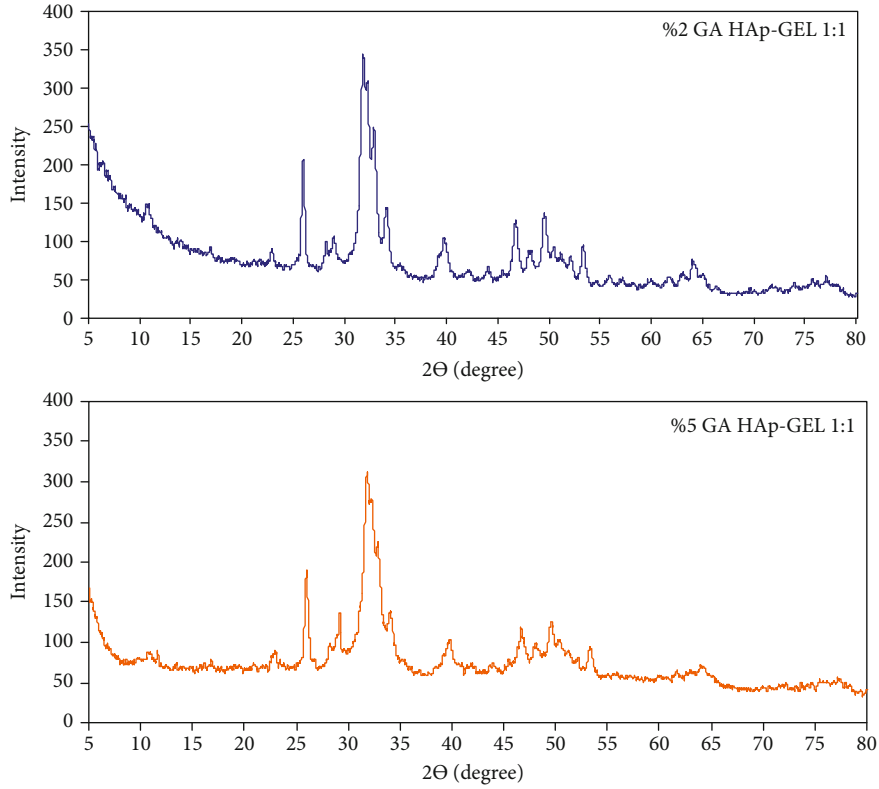

Figure 2: XRD patterns of the HAp-GEL composites cross-linked with different amounts of GA.

The GEL ratio was higher in the HAp-GEL 5% GA composite. Thermal, mechanical, and moisture resistance can be increased by forming covalent bonds between aldehyde-based cross-linking agents and GEL chains [79]. By increasing the amount of the cross-linking agent, the proportion of GEL remaining dissolved in the SBF and removed by filtration could be reduced during the composite production stage. In this way, the amount of GEL interacting with HAp increased. The increase in the amount of GEL retained in the composite along with the increased amount of cross-linking agent was confirmed by TGA.

3.3. FTIR Analysis of the HAp-GEL Composites. Figure 4 shows the FTIR patterns of HAp, GEL, 5-FU, and the loaded and unloaded HAp-GEL 2% GA and HAp-GEL 5% GA composites. For the HAp-GEL 2% GA composite, the PO_4 bands were observed around 1020.39°cm^{-1} in the $\upsilon 3$ mode and 961.56°cm^{-1} in the $\upsilon 1$ mode, indicating the presence of the HAp phase. For HAp-GEL 5% GA, PO_4 bands were seen around 1018.46 in the $\upsilon 3$ mode and ~900 in the $\upsilon 1$ mode. The bands between 3000°cm^{-1} and 3600°cm^{-1} were caused by O-H stretching and are characteristic HAp peaks. Typical H-O-H bands were observed between 3680°cm^{-1} and 3840°cm^{-1} in all composites, which may be caused by the binding energies of free water molecules on the HAp surface. The 1422.56°cm^{-1} band in the $\upsilon 3$ mode and the 873.79°cm^{-1} band in the $\upsilon 2$ mode in the HAp-GEL 2% GA composite and the 1419.67°cm^{-1} band in the $\upsilon 3$ mode and the 874.76°cm^{-1} band in the $\upsilon 2$ mode in the HAp-GEL 5% GA composite indicated the presence of CO_3 ions. Amide I and amide II bands were observed around 1650.17°cm^{-1} and 1545.05°cm^{-1} for HAp-GEL 2% GA and at 1641.49°cm^{-1} and 1536.37cm^{-1} for HAp-GEL 5% GA. These are related to the presence of GEL [46, 51, 80, 81].

In Figures 4(b) and 4(c), new 5-FU peaks emerge in the loaded composites, as expected. Some extra bands attributed to 5-FU and ions in the SBF are observed. Around 1400 cm^{-1} (aromatic ring), which overlaps with the band of CO_3 ions, the bands at 870 cm^{-1} (CF=CH groups) and 3000-3500 cm^{-1} (unbonded F group) show the encapsulation of 5-FU [82]. Moreover, the band at 870 cm^{-1} could be attributed to the FNO_3 structure [83]. Regarding the sample with GA, no significant differences within the sample cross-linked with GA were observed (Figure 4). A comparison among the samples with different amounts of GA showed that the intensities of the amid I and II bands (around 1650 cm^{-1} and 1550 cm^{-1}) increased with the increase in the GA ratio. This situation could be confirmed using the TGA results (Figure 3).

3.4. SEM Analysis of the Drug-Loaded HAp-GEL Composites. SEM images of the drug-loaded HAp-GEL composites are illustrated in Figures 5(a) and 5(b). For each composite, drug-loaded spherical particles were observed. However, similar to the morphology of pure gelatin, adjacent spherical particles were also observed. Agglomerated irregular shapes can be caused by impurities [54, 84, 85]. In general, a regular particle size distribution was not observed.

SEM images of the unloaded HAp-GEL composites are shown in Figures 5(c) and 5(d). In Figure 5(d), HAp whiskers

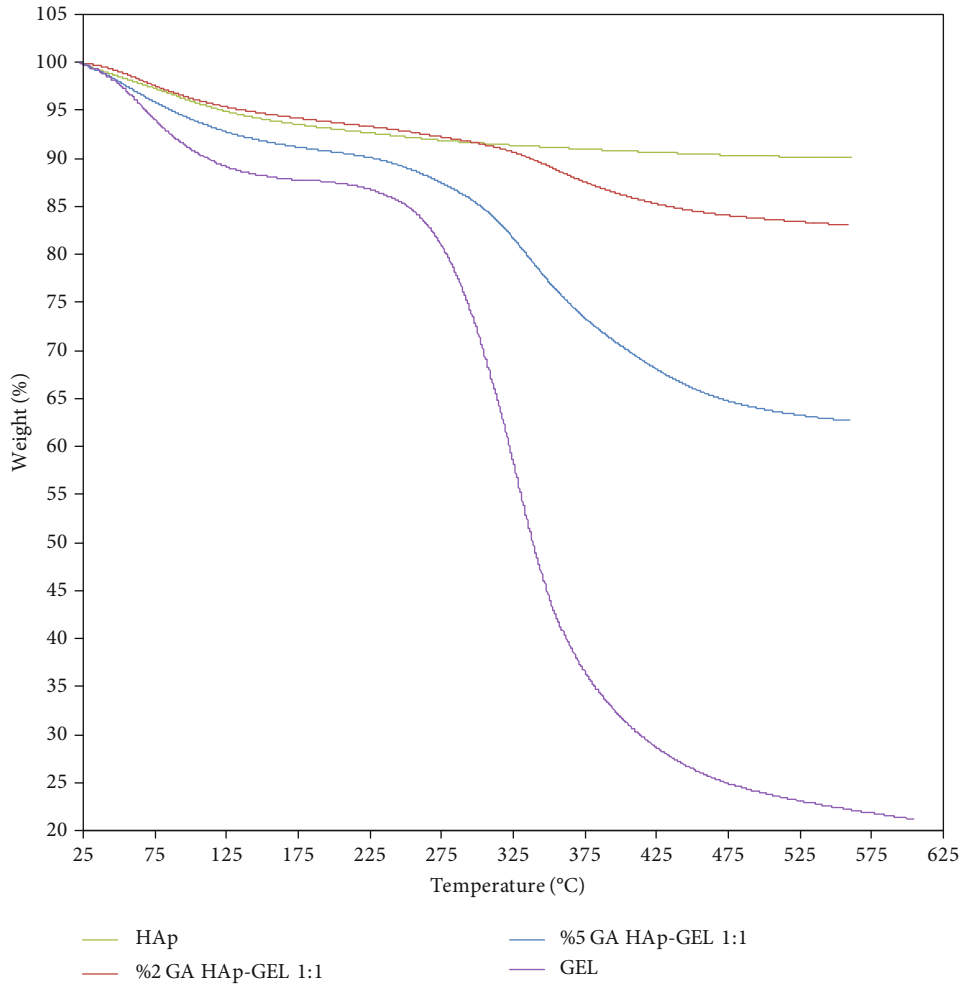

Figure 3: TGA patterns of pure HAp, pure gelatin, and the HAp-GEL composites cross-linked with different amounts of GA.

and hexagonal crystal structures are observed, which is a sign of HAp crystal formation [86].

3.5. Drug Release Profiles of the HAp-GEL Composites. The drug release profiles of the HAp-GEL composites with drug loaded by spray drying were evaluated at three different temperatures (32°C, 37°C, and 42°C) according to three different kinetic models. The release profiles of the HAp-GEL 2% GA and HAp-GEL 5% GA are illustrated in Figure 6. A biphasic release profile is observed in all composites. The drug release data for the 2% GA and 5% GA composites (HAp-GEL-5-FU) at 32°C shows that within the first 5 min, 40% and 35% of 5-FU are released, respectively. For the 2% GA and 5% GA composites, 55% and 50% of 5-FU were released at 37°C and 75% and 60% at 42°C within 5 min, respectively. This rapid initial release rate has been attributed to either the presence of nonencapsulated drug molecules on the surface of the microparticles or drug molecules that are close to the surface (immersed in the polymer matrix) [70]. For the 2% GA and 5% GA composites, the drug was almost completely released from the composites within 60 and 180 minutes, respectively. For HAp-GEL composites, the initial burst increased with increasing temperature. Shirakura et al. studied the drug release behavior of cisplatin in hydrogel nanoparticles with changing temperature, and the highest amount of drug release was observed at 42°C. This result was attributed to the fact that the matrix density decreased because of the swelling of the nanoparticles at higher temperatures, thus facilitating the escape of cisplatin. In addition, the diffusion rate of cisplatin might have been increased with increasing temperature [64].

Similarly, the same results were observed in other temperature-controlled studies. Thus, increasing temperature can cause the escape of 5-FU molecules from HAp-GEL composites, and the diffusion rate of 5-FU may be affected by temperature [65–67]. In this study, during the entire release process, the release rate and cumulative release percentage were affected by the temperature, while the diffusion rate of 5-FU was affected by the molecular thermal motion [70, 87]. As seen in Figure 6, all HAp-GEL composites showed an initial burst and a 50% drug release in 20-25 minutes. In physiological environments, 5-FU has a half-life of approximately 8-20 minutes [88].

Figure 7 shows the drug release profiles of HAp-GEL composites with different amounts of GA at three different temperatures (32°C, 37°C, and 42°C). At each temperature,

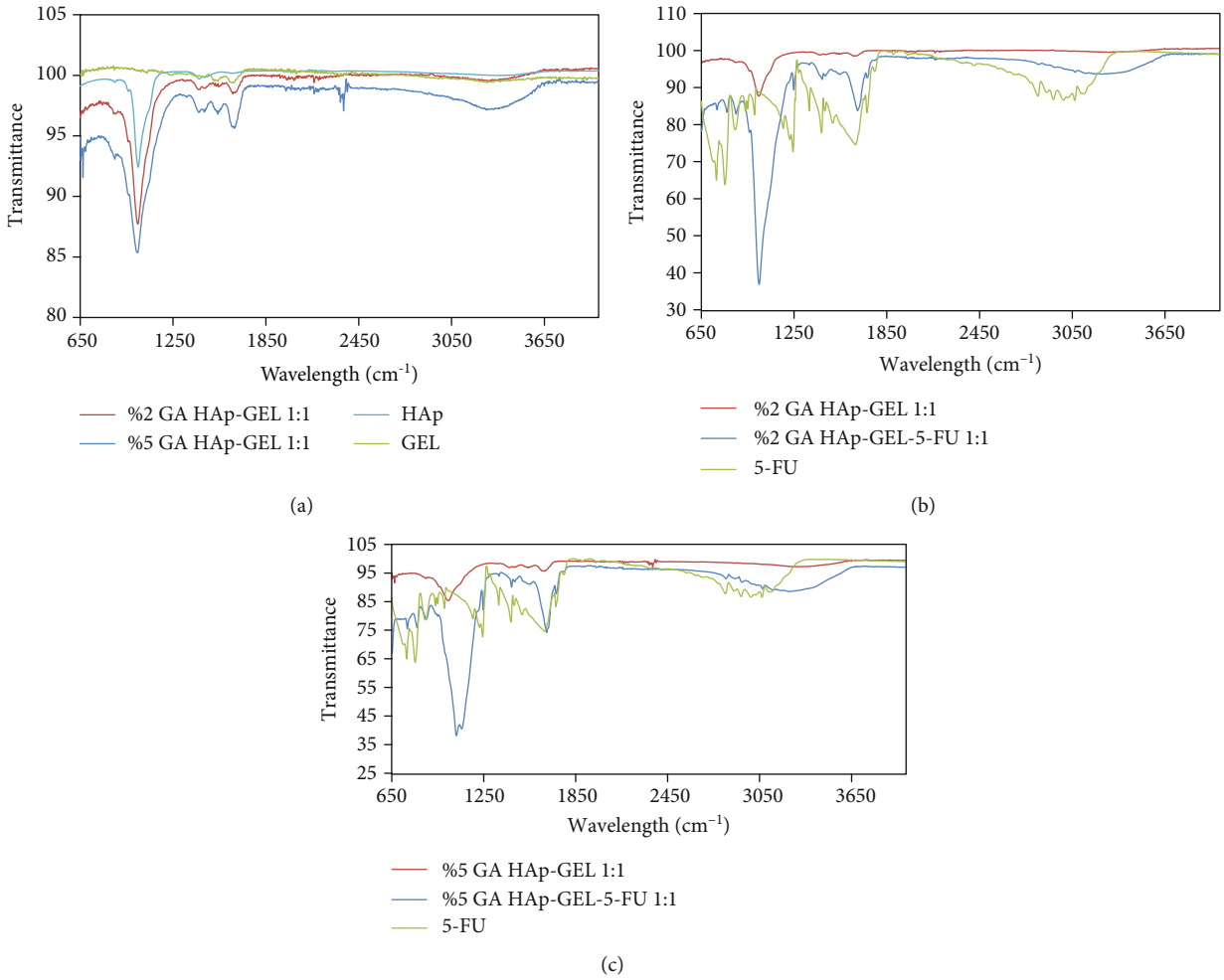

Figure 4: FTIR patterns of (a) the HAp-GEL composites cross-linked with different amounts of GA, pure HAp, and pure GEL; (b) the drug-loaded and unloaded 2% GA HAp-GEL composites, pure 5-FU; and (c) the drug-loaded and unloaded 5% GA HAp-GEL composites, pure 5-FU.

similar initial burst values are obtained. It is observed that the release rate increases with increasing temperature. This result is in agreement with the literature [70, 87, 89, 90].

Because HAp-GEL with a 1 : 1 weight ratio had the highest drug loading efficiency [91], drug release studies were conducted on that sample for different GA ratios. A burst release was observed in all samples during the first hour. For the HAp-GEL composites, the initial burst decreased with increasing GA content at all three temperatures. In other words, the drug release from HAp-GEL-5-FU 5% GA was slower than that from the HAp-GEL-5-FU 2% GA. The diffusion rate and quantity of drug release from the polymer matrix were influenced by the cross-linker ratio [92]. Similarly, Kim et al. and Peng et al. reported that increasing the GA content decreased the initial burst in a GEL microsphere and GEL-HAp nanocomposite, respectively [39, 46]. Burst releases may be related to some drugs being weakly bonded to the surface of the composites [93]. According to the work of Santos, the release of 5-FU from spray-dried HAp was accomplished in the first 5 min [54]. Based on the literature, the 5-FU release from GEL is slower and/or less than the drug release from HAp [46, 94] Moreover, the addition of GA reduces the drug release because of the increased rigidity in polymer chains [51, 93]. Thus, it may be concluded that the addition of GEL and GA to HAp in the presence of an SBF may slow down the burst release. Overall, the release of the anticancer drug occurred in a slow manner, and these HAp-polymer composites could be used for controlled and sustained drug release [92].

Mathematical models of drug release could provide useful information about the mass transfer responsible for drug delivery system. They also reveal the influence of important parameters, such as morphology and loading of encapsulated materials on the release rate [87]. To better understand the release mechanism of 5-FU encapsulated in HAp-GEL, three different fitting equations, including zero order, first order, and Higuchi models, were used to fit the release curve. The kinetic mathematical model and the fitting results for the drug release at different temperatures are shown in Table 2. It is found that the release profile of 5-FU from the drug-loaded HAP-GEL polymer composites is best fitted by the Higuchi model with the highest value of regression

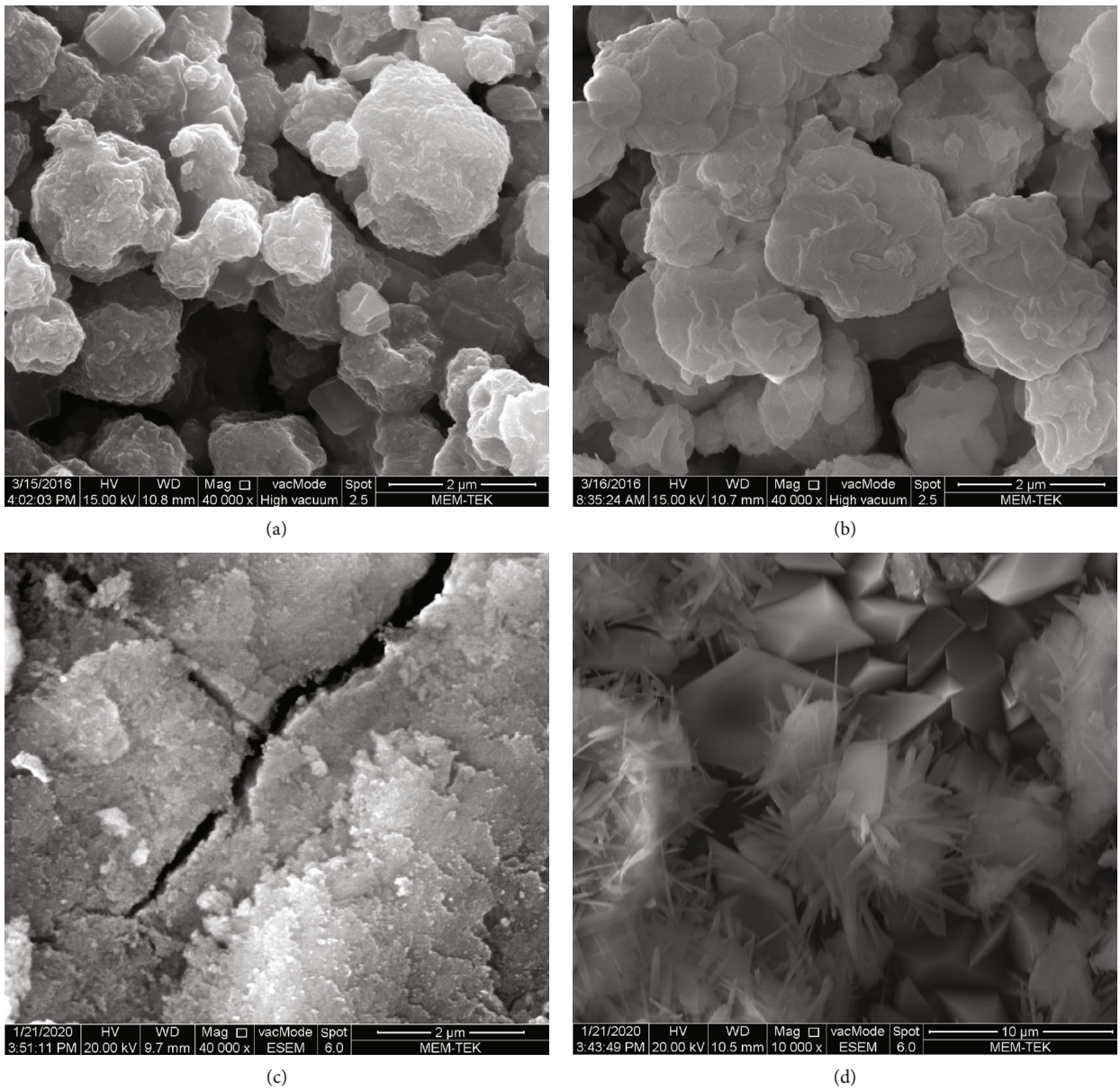

Figure 5: SEM images of (a) HAp-GEL-5-FU 2% GA, (b) HAp-GEL-5-FU 5% GA, (c) HAp-GEL 2% GA, and (d) HAp-GEL 5% GA.

coefficients (R^2). Nevertheless, for HAp-GEL 2% GA at 37°C, the regression coefficient ($R^2 = 0.955$) is close to 1. This indicates that diffusion is dominated by Fickian diffusion mechanism [82, 95–97]. This is commonly observed in calcium phosphates (CaPs) and CaP cements. Moreover, this type of diffusion of 5-FU was also observed in other studies related to gelatin and chitosan polymers [51, 82]. For HAp-GEL 2% GA at 32°C and 42°C and HAp-GEL 5% GA at 32°C, 37°C, and 42°C, the regression coefficients (R^2 was 0.817, 0.891, 0.934, 0.747, and 0.905, respectively) were lower than 1. For this reason, the release of 5-FU from the HAp-GEL polymer composites occurred through non-Fickian diffusion mechanisms in most cases. All sample releases are in accordance with the Higuchi model, which is diffusion-controlled [68–72, 92].

4. Conclusion

The current study focused on the preparation of 5-FU-loaded HAp-GEL polymer composites and their in vitro drug release in a PBS medium at different temperatures. The HAp-GEL composites were produced using wet chemical precipitation, and the encapsulation (drug loading) process of 5-FU was conducted in a spray dryer. The obtained composites were characterized by XRD, TGA, FTIR, and SEM.

According to XRD and FTIR analysis, formation of hydroxyapatite crystals was confirmed. To observe the effect of temperature on the drug release mechanism, in vitro drug release studies were conducted at 32°C, 37°C, and 42°C and pH 4.0 in a PBS medium. For the HAp-GEL composites, the initial burst increased with increasing temperature. Two

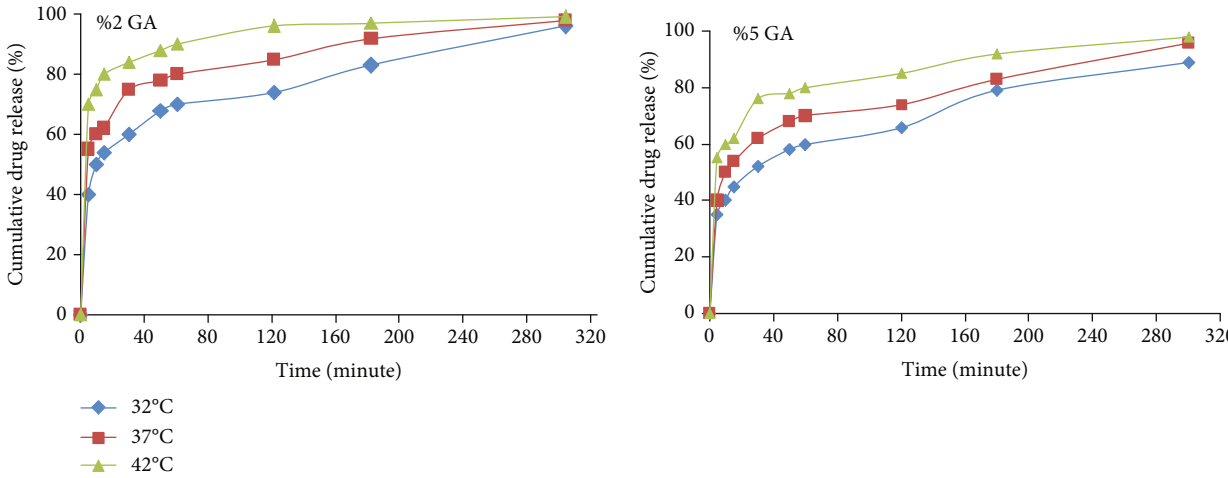

Figure 6: Drug release profiles of the HAp-GEL composites with changing temperature.

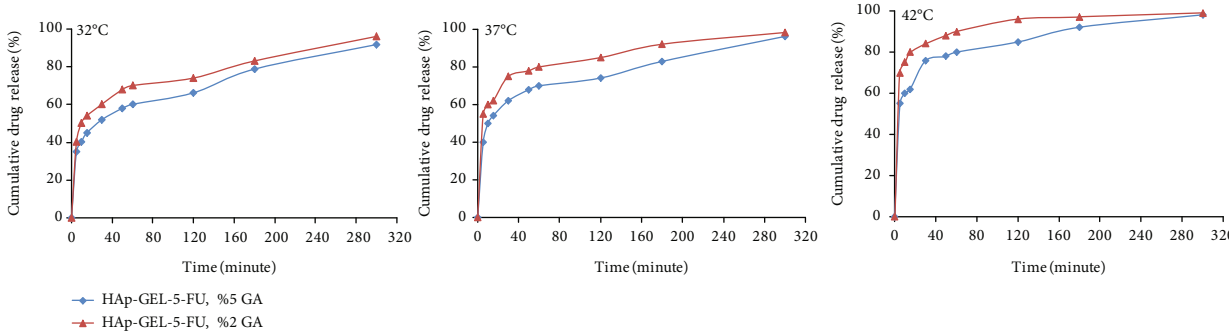

Figure 7: Drug release profiles of the HAp-GEL composites with changing GA values at 32°C, 37°C, and 42°C.

Table 2: Kinetic parameters (R^2, K_0, K, and K_H) of various models for the release of 5-FU from the drug-loaded HAp-GEL polymer composites.

Release temperature	Composites	Zero order		First order		Higuchi	
		K_0	R^2	K	R^2	K_H	R^2
32°C	HAp-GEL, 2% GA	0.134	0.674	0.310	0.279	41.20	0.817
37°C		0.220	0.837	0.280	0.331	11.60	0.955
42°C		0.120	0.831	0.150	0.299	6.50	0.891
32°C	HAp-GEL, 5% GA	0.125	0.825	0.300	0.824	40.60	0.934
37°C		0.200	0.569	0.240	0.297	10.50	0.747
42°C		0.101	0.762	0.130	0.243	6.01	0.905

different cross-linking solutions of 5% and 2% GA-deionized water (*v*/*v*) were used during the preparation of the microparticles to understand the effect of the GA amount. For the HAp-GEL composites, the initial burst decreased with increasing GA content at all three temperatures. These results are in accordance with those of previous studies.

The drug release profiles were evaluated according to three different kinetic models including zero order, first order, and Higuchi. In the kinetic model studies, the highest correlation values (R^2) were observed for the Higuchi model equation of diffusion, demonstrating that the drug release was proportional to the square root of time and occurred through diffusion. The HAp-GEL polymer composites occurred through non-Fickian diffusion mechanisms, with only one exception. Among the three kinetic studies investigated, it was determined that all composites best fit the Higuchi model. These polymer composites will be biocompatible and biodegradable, thus could be applied to controlled and sustained drug delivery systems.

Data Availability

All raw data used to support the findings of this study are available from the corresponding author upon request.

Conflicts of Interest

The author declares that there is no conflict of interest regarding the publication of this paper.

References

[1] A. Szcześ, L. Hołysz, and E. Chibowski, "Synthesis of hydroxyapatite for biomedical applications," *Advances in Colloid and Interface Science*, vol. 249, pp. 321–330, 2017.

[2] D. Rădulescu, V. Grumezescu, E. Andronescu et al., "Biocompatible cephalosporin-hydroxyapatite-poly(lactic-co-glycolic acid)-coatings fabricated by MAPLE technique for the prevention of bone implant associated infections," *Applied Surface Science*, vol. 374, pp. 387–396, 2016.

[3] L. An, W. Li, Y. Xu, D. Zeng, Y. Cheng, and G. Wang, "Controlled additive-free hydrothermal synthesis and characterization of uniform hydroxyapatite nanobelts," *Ceramics International*, vol. 42, no. 2, pp. 3104–3112, 2016.

[4] M. N. Hassan, M. M. Mahmoud, and A. A. El-Fattah, "Microwave-assisted preparation of Nano-hydroxyapatite for bone substitutes," *Ceramics International*, vol. 42, no. 3, pp. 3725–3744, 2016.

[5] M. Supova, "Substituted hydroxyapatites for biomedical applications: a review," *Ceramics International*, vol. 41, no. 8, pp. 9203–9231, 2015.

[6] J. Yan, Y. Miao, H. Tan et al., "Injectable alginate/hydroxyapatite gel scaffold combined with gelatin microspheres for drug delivery and bone tissue engineering," *Materials Science and Engineering: C*, vol. 63, pp. 274–284, 2016.

[7] S. Sathiyavimal, S. Vasantharaj, F. LewisOscar, A. Pugazhendhi, and R. Subashkumar, "Biosynthesis and characterization of hydroxyapatite and its composite (hydroxyapatite-gelatin-chitosan-fibrin-bone ash) for bone tissue engineering applications," *International Journal of Biological Macromolecules*, vol. 129, pp. 844–852, 2019.

[8] S. Chen, Y. Shi, Y. Luo, and J. Ma, "Layer-by-layer coated porous 3D printed hydroxyapatite composite scaffolds for controlled drug delivery," *Colloids and Surfaces B: Biointerfaces*, vol. 179, pp. 121–127, 2019.

[9] S. Jinawath, D. Pongkao, and M. Yoshimura, "Hydrothermal synthesis of hydroxyapatite from natural source," *Journal of Materials Science: Materials in Medicine*, vol. 13, no. 5, pp. 491–494, 2012.

[10] Y. Wang, S. Zhang, K. Wei, N. Zhao, J. Chen, and X. Wang, "Hydrothermal synthesis of hydroxyapatite nanopowders using cationic surfactant as a template," *Materials Letters*, vol. 60, no. 12, pp. 1484–1487, 2006.

[11] W. Feng, L. Mu-sen, L. Yu-peng, and Q. Yong-xin, "A simple sol-gel technique for preparing hydroxyapatite nanopowders," *Materials Letters*, vol. 59, no. 8-9, pp. 916–919, 2005.

[12] G. C. Koumoulidis, A. P. Katsoulidis, A. K. Ladavos et al., "Preparation of hydroxyapatite via microemulsion route," *Journal of Colloid and Interface Science*, vol. 259, no. 2, pp. 254–260, 2003.

[13] I. Mobasherpour, M. S. Heshajin, A. Kazemzadeh, and M. Zakeri, "Synthesis of nanocrystalline hydroxyapatite by using precipitation method," *Journal of Alloys and Compounds*, vol. 430, no. 1-2, pp. 330–333, 2007.

[14] R. R. Rao, H. N. Roopa, and T. S. Kannan, "Solid state synthesis and thermal stability of HAP and HAP–β-TCP composite ceramic powders," *Journal of Materials Science: Materials in Medicine*, vol. 8, no. 8, pp. 511–518, 1997.

[15] P. Parhi, A. Ramanan, and A. R. Ray, "A convenient route for the synthesis of hydroxyapatite through a novel microwave-mediated metathesis reaction," *Materials Letters*, vol. 58, no. 27-28, pp. 3610–3612, 2004.

[16] R. H. Bhowmik, K. S. Katti, and D. Katti, "Molecular dynamics simulation of hydroxyapatite–polyacrylic acid interfaces," *Polymer*, vol. 48, no. 2, pp. 664–674, 2007.

[17] S. C. Chao, M. J. Wang, N. S. Pai, and S. K. Yen, "Preparation and characterization of gelatin-hydroxyapatite composite microspheres for hard tissue repair," *Materials Science and Engineering: C*, vol. 57, pp. 113–122, 2015.

[18] M. Ito, Y. Hidaka, M. Nakajima, H. Yagasaki, and A. H. Kafrawy, "Effect of hydroxyapatite content on physical properties and connective tissue reactions to a chitosan–hydroxyapatite composite membrane," *Journal of Biomedical Materials Research*, vol. 45, no. 3, pp. 204–208, 1999.

[19] J. F. Mano, C. M. Vaz, S. C. Mendes, R. L. Reis, and A. M. Cunha, "Dynamic mechanical properties of hydroxyapatite-reinforced and porous starch-based degradable biomaterials," *Journal of Materials Science: Materials in Medicine*, vol. 10, no. 12, pp. 857–862, 1999.

[20] M. B. Yaylaoglu, P. Korkusuz, U. Ors, F. Korkusuz, and V. Hasirci, "Development of a calcium phosphate–gelatin composite as a bone substitute and its use in drug release," *Biomaterials*, vol. 20, no. 8, pp. 711–719, 1999.

[21] A. Tempieri, M. Sandri, E. Landi et al., "A convenient route for the synthesis of hydroxyapatite through a novel microwave-mediated metathesis reaction," *Acta Biomaterialia*, vol. 1, pp. 343–351, 2005.

[22] Y. Zhai and F. Z. Cui, "Recombinant human-like collagen directed growth of hydroxyapatite nanocrystals," *Journal of Crystal Growth*, vol. 291, no. 1, pp. 202–206, 2006.

[23] B. Shalini and A. R. Kumar, "Preparation And Characterisation Of Gelatin Blend Pectin Encapsulated Hydroxyapatite ($Ca_{10}(OH)_2(PO_4)_6$) Nanoparticles Using Precipitation Method," *Materials Today: Proceedings*, vol. 8, pp. 245–249, 2019.

[24] M. Rahmanian, A. Seyfoori, M. M. Dehghan et al., "Multifunctional gelatin-tricalcium phosphate porous nanocomposite scaffolds for tissue engineering and local drug delivery: *In vitro* and *in vivo* studies," *Journal of the Taiwan Institute of Chemical Engineers*, vol. 101, pp. 214–220, 2019.

[25] N. Ashwanikumar, N. A. Kumar, S. A. Nair, and G. S. V. Kumar, "Dual drug delivery of 5-fluorouracil (5-FU) and methotrexate (MTX) through random copolymeric nanomicelles of PLGA and polyethylenimine demonstrating enhanced cell uptake and cytotoxicity," *Colloids and Surfaces B: Biointerfaces*, vol. 122, pp. 520–528, 2014.

[26] A. Touny, C. Laurencin, L. Nair, H. Allcock, and P. W. Brown, "Formation of composites comprised of calcium deficient HAp and cross-linked gelatin," *Journal of Materials Science: Materials in Medicine*, vol. 19, no. 10, pp. 3193–3201, 2008.

[27] A. Bigi, M. Borghi, G. Cojazzi, A. M. Fivhera, S. Panzavolta, and N. Roveri, "Structural and mechanical properties of cross-linked drawn gelatin films," *Journal of Thermal Analysis and Calorimetry*, vol. 61, no. 2, pp. 451–459, 2000.

[28] A. Yao, B. Liu, C. Chang, S. Hsu, and Y. Chen, "Preparation of networks of gelatin and genipin as degradable biomaterials,"

Materials Chemistry and Physics, vol. 83, no. 2-3, pp. 204–208, 2004.

[29] M. Usta, D. L. Piech, R. K. MacCrone, and W. B. Hillig, "Behavior and properties of neat and filled gelatins," *Biomaterials*, vol. 24, no. 1, pp. 165–172, 2003.

[30] T. Bera, A. N. Vivek, S. K. Saraf, and P. Ramachandrarao, "Characterization of biomimetically synthesized HAp-GEL nanocomposites as bone substitute," *Biomedical Materials*, vol. 3, no. 2, p. 025001, 2008.

[31] T. A. Esquivel-Castro, M. C. Ibarra-Alonso, J. Oliva, and A. Martínez-Luévanos, "Porous aerogel and core/shell nanoparticles for controlled drug delivery: a review," *Materials Science and Engineering C*, vol. 96, pp. 915–940, 2019.

[32] J. Chen and F. Chang, "Preparation and characterization of hydroxyapatite/gelatin composite membranes for immunoisolation," *Applied Surface Science*, vol. 262, pp. 176–183, 2012.

[33] F. Ghorbani, H. Nojehdehian, and A. Zamanian, "Physicochemical and mechanical properties of freeze cast hydroxyapatite- gelatin scaffolds with dexamethasone loaded PLGA microspheres for hard tissue engineering applications," *Materials Science and Engineering C*, vol. 69, pp. 208–220, 2016.

[34] H. Ture, "Characterization of hydroxyapatite-containing alginate-gelatin composite films as a potential wound dressing," *International Journal of Biological Macromolecules*, vol. 123, pp. 878–888, 2019.

[35] J. Xiao, Y. Zhu, Y. Liu, Y. Zeng, and F. Xu, "An asymmetric coating composed of gelatin and hydroxyapatite for the delivery of water insoluble drug," *Journal of Materials Science: Materials in Medicine*, vol. 20, no. 4, pp. 889–896, 2009.

[36] M. Stigter, J. Bezemer, K. Groot, and P. Layrolle, "Incorporation of different antibiotics into carbonated hydroxyapatite coatings on titanium implants, release and antibiotic efficacy," *Journal of Controlled Release*, vol. 99, no. 1, pp. 127–137, 2004.

[37] Y.-L. Lai, P.-Y. Cheng, C.-C. Yang, and S.-K. Yen, "Electrolytic deposition of hydroxyapatite/calcium phosphate-heparin/-gelatin- heparin tri-layer composites on NiTi alloy to enhance drug loading and prolong releasing for biomedical applications," *Thin Solid Films*, vol. 649, pp. 192–201, 2018.

[38] S. Teng, L. Chen, Y. Guo, and J. Shi, "Formation of nanohydroxyapatite in gelatin droplets and the resulting porous composite microspheres," *Journal of Inorganic Biochemistry*, vol. 101, no. 4, pp. 686–691, 2007.

[39] H. W. Kim, J. C. Knowles, and H. E. Kim, "Porous scaffolds of gelatin-hydroxyapatite nanocomposites obtained by biomimetic approach: characterization and antibiotic drug release," *Journal of Biomedical Materials Research Part B: Applied Biomaterials*, vol. 74B, no. 2, pp. 686–698, 2005.

[40] X. C. Dou, X. P. Zhu, J. Zhou, H. Q. Cai, J. Tang, and Q. L. Li, "Minocycline-released hydroxyapatite–gelatin nanocomposite and its cytocompatibilityin vitro," *Biomedical Materials*, vol. 6, no. 2, p. 025002, 2011.

[41] M. Sivakumar and K. P. Rao, "Preparation, characterization and in vitro release of gentamicin from coralline hydroxyapatite-gelatin composite microspheres," *Biomaterials*, vol. 23, no. 15, pp. 3175–3181, 2002.

[42] W. Yu, G. Jiang, D. Liu, Z. Tong, J. Yao, and X. Kong, "Transdermal delivery of insulin with bioceramic composite microneedles fabricated by gelatin and hydroxyapatite," *Materials Science and Engineering C*, vol. 73, pp. 425–428, 2017.

[43] F. Fayyazbakhsh, M. Solati-Hashjin, A. Keshtkar, M. A. Shokrgozar, M. M. Dehghan, and B. Larijani, "Release behavior and signaling effect of vitamin D3 in layered double hydroxides-hydroxyapatite/gelatin bone tissue engineering scaffold: An in vitro evaluation," *Colloids and Surfaces B: Biointerfaces*, vol. 158, pp. 697–708, 2017.

[44] M. Olukman, O. Sanlı, and E. K. Solak, "Release of anticancer drug 5-fluorouracil from different Ionically Crosslinked alginate beads," *Journal of Biomaterials and Nanobiotechnology*, vol. 3, no. 4, pp. 469–479, 2012.

[45] T. He, W. Wang, B. Chen, J. Wang, Q. Liang, and B. Chen, "5-Fluorouracil monodispersed chitosan microspheres: Microfluidic chip fabrication with crosslinking, characterization, drug release and anticancer activity," *Carbohydrate Polymers*, vol. 236, article 116094, 2020.

[46] Z. Peng, Z. Li, and Y. Shen, "Preparation and in vitro characterization of gelatin microspheres containing 5-fluorouracil," *Journal of Macromolecular Science, Part B*, vol. 51, no. 6, pp. 1117–1124, 2012.

[47] R. L. Sastre, R. Olmo, C. Teijon, E. Munız, J. M. Teijon, and M. D. Blanco, "5-Fluorouracil plasma levels and biodegradation of subcutaneously injected drug-loaded microspheres prepared by spray-drying poly(d,l-lactide) and poly(d,l-lactide-co-glycolide) polymers," *International Journal of Pharmaceutics*, vol. 338, no. 1-2, pp. 180–190, 2007.

[48] E. Fournier, C. Passirani, N. Colin, P. Breton, S. Sagodira, and J. Benoit, "Development of novel 5-FU-loaded poly(methylidene malonate 2.1.2)-based microspheres for the treatment of brain cancers," *European Journal of Pharmaceutics and Biopharmaceutics*, vol. 57, no. 2, pp. 189–197, 2004.

[49] R. K. Dutta and S. Sahu, "Development of a novel probe sonication assisted enhanced loading of 5-FU in SPION encapsulated pectin nanocarriers for magnetic targeted drug delivery system," *European Journal of Pharmaceutics and Biopharmaceutics*, vol. 82, no. 1, pp. 58–65, 2012.

[50] Y. Lin, Y. Li, and C. P. Ooi, "5-Fluorouracil encapsulated HA/PLGA composite microspheres for cancer therapy," *Journal of Materials Science: Materials in Medicine*, vol. 23, no. 10, pp. 2453–2460, 2012.

[51] Z. Zhou, L. Liu, Q. Liu et al., "Study on controlled release of 5-fluorouracil from gelatin/chitosan microspheres," *Journal of Macromolecular Science, Part A: Pure and Applied Chemistry*, vol. 49, no. 12, pp. 1030–1034, 2012.

[52] A. Dalmoro, A. Y. Sitenkov, S. Cascone, G. Lamberti, A. A. Barba, and R. I. Moustafine, "Hydrophilic drug encapsulation in shell-core microcarriers by two stage polyelectrolyte complexation method," *International Journal of Pharmaceutics*, vol. 518, no. 1-2, pp. 50–58, 2017.

[53] T. S. Anirudhan and J. Christa, "Temperature and pH sensitive multi-functional magnetic nanocomposite for the controlled delivery of 5-fluorouracil, an anticancer drug," *Journal of Drug Delivery Science and Technology*, vol. 55, article 101476, 2020.

[54] C. Santos, C. F. Rovath, R. P. Franke, M. M. Almeida, and M. E. V. Costa, "Spray-dried hydroxyapatite-5-fluorouracil granules as a chemotherapeutic delivery system," *Ceramics International*, vol. 35, no. 1, pp. 509–513, 2009.

[55] R. A. Bader and D. A. Putnam, *Engineering Polymer Systems for Improved Drug Delivery*, John Wiley & Sons, Inc., New York, 2014.

[56] D. Suvakanta, P. N. Murthy, L. Nath, and P. Chowdhury, "Kinetic model on drug release from controlled drug delivery systems," *Acta Poloniae Pharmaceutica n Drug Research*, vol. 67, no. 3, pp. 217–223, 2010.

[57] M. Mucalo, *Hydroxyapatite (HAp) for biomedical applications*, Elsevier, 2015.

[58] W. Xu, Y. Hong, A. Song, and J. Hao, "Peptide-assembled hydrogels for pH-controllable drug release," *Colloids and Surfaces B: Biointerfaces*, vol. 185, article 110567, 2020.

[59] Y. Xu, D. Liu, J. Hu, P. Ding, and M. Chen, "Hyaluronic acid-coated pH sensitive poly (β-amino ester) nanoparticles for co- delivery of embelin and TRAIL plasmid for triple negative breast cancer treatment," *International Journal of Pharmaceutics*, vol. 573, article 118637, 2020.

[60] C. Ding, H. Wu, Z.-Z. Yin et al., "Disulfide-cleavage- and pH-triggered drug delivery based on a vesicle structured amphiphilic self-assembly," *Materials Science and Engineering: C*, vol. 107, article 110366, 2020.

[61] J. Wang, N. Huang, Q. Peng, X. Cheng, and W. Li, "Temperature/pH dual-responsive and luminescent drug carrier based on PNIPAM- MAA/lanthanide-polyoxometalates for controlled drug delivery and imaging in HeLa cells," *Materials Chemistry and Physics*, vol. 239, article 121994, 2020.

[62] Y. Yun, H. Wu, J. Gao et al., "Facile synthesis of Ca^{2+}-cross-linked sodium alginate/graphene oxide hybrids as electro- and pH-responsive drug carrier," *Materials Science and Engineering: C*, vol. 108, article 110380, 2020.

[63] E. Benova, D. Berge-Lefranc, V. Zelenak, M. Almasi, V. Huntosova, and V. Hornebecq, "Adsorption properties, the pH-sensitive release of 5-fluorouracil and cytotoxicity studies of mesoporous silica drug delivery matrix," *Applied Surface Science*, vol. 504, article 144028, 2020.

[64] T. Shirakura, T. J. Kelson, A. Ray, A. E. Malyarenko, and R. Kopelman, "Hydrogel nanoparticles with thermally controlled drug release," *ACS Macro Letters*, vol. 3, no. 7, pp. 602–606, 2014.

[65] A. Externbrink, M. R. Clark, D. R. Friend, and S. Klein, "Investigating the feasibility of temperature-controlled accelerated drug release testing for an intravaginal ring," *European Journal of Pharmaceutics and Biopharmaceutics*, vol. 85, no. 3, pp. 966–973, 2013.

[66] Z. Al-Ahmady, M. Hadjidemetriou, J. Gubbins, and K. Kostarelos, "Formation of protein corona in vivo affects drug release from temperature- sensitive liposomes," *Journal of Controlled Release*, vol. 276, pp. 157–167, 2018.

[67] V. Brunella, S. A. Jadhav, I. Miletto et al., "Hybrid drug carriers with temperature-controlled on-off release: A simple and reliable synthesis of PNIPAM-functionalized mesoporous silica nanoparticles," *Reactive and Functional Polymers*, vol. 98, pp. 31–37, 2016.

[68] Z. Li, M. Cai, K. Yang, and P. Sun, "Kinetic study of d-limonene release from finger citron essential oil loaded nanoemulsions during simulated digestion in vitro," *Journal of Functional Foods*, vol. 58, pp. 67–73, 2019.

[69] A. Rasool, S. Ata, A. Islam et al., "Kinetics and controlled release of lidocaine from novel carrageenan and alginate-based blend hydrogels," *International Journal of Biological Macromolecules*, vol. 147, pp. 67–78, 2020.

[70] N. Pettinelli, S. Rodríguez-Llamazares, Y. Farrag et al., "Poly(-hydroxybutyrate- co -hydroxyvalerate) microparticles embedded in κ-carrageenan/locust bean gum hydrogel as a dual drug delivery carrier," *International Journal of Biological Macromolecules*, vol. 146, pp. 110–118, 2020.

[71] H. K. Shaikh, R. V. Kshirsagar, and S. G. Patil, "Mathematical model for drug release characterization: a review," *World Journal of Phrmacy and Pharmaceutical Sciences*, vol. 4, pp. 324–338, 2015.

[72] A. Di Martino, A. Drannikov, N. S. Surgutskaia et al., "Chitosan-collagen based film for controlled delivery of a combination of short life anesthetics," *International Journal of Biological Macromolecules*, vol. 140, pp. 1183–1193, 2019.

[73] H. S. Kim, J. T. Kim, Y. J. Yung, S. C. Ryu, H. J. Son, and Y. G. Kim, "Preparation of a porous chitosan/fibroin-hydroxyapatite composite matrix for tissue engineering," *Macromolecular Research*, vol. 15, no. 1, pp. 65–73, 2007.

[74] S. W. K. Kweh, K. A. Khor, and P. Cheang, "The production and characterization of hydroxyapatite (HA) powders," *Journal of Materials Processing Technology*, vol. 89-90, pp. 373–377, 1999.

[75] C. Shu, Y. Xianzhu, X. Zhangyin, X. Guohua, L. Hong, and Y. Kangde, "Synthesis and sintering of nanocrystalline hydroxyapatite powders by gelatin- based precipitation method," *Ceramics International*, vol. 33, no. 2, pp. 193–196, 2007.

[76] S. Tummala, M. N. S. Kumar, and A. Prakash, "Formulation and characterization of 5-fluorouracil enteric coated nanoparticles for sustained and localized release in treating colorectal cancer," *Saudi Pharmaceutical Journal*, vol. 23, no. 3, pp. 308–314, 2015.

[77] K. R. Aubrey and R. J. Vandenberg, "Glycine transport inhibitors as potential antipsychotic drugs," *Expert Opinion on Therapeutic Targets*, vol. 5, no. 4, pp. 507–518, 2001.

[78] X. Fenglan, L. Yubao, W. Xuejiang, W. Jie, and Y. Aiping, "Preparation and characterization of nano-hydroxyapatite/-poly (vinyl alcohol) hydrogel biocomposite," *Journal of Materials Science*, vol. 39, no. 18, pp. 5669–5672, 2004.

[79] M. C. Chang, W. H. Douglas, and J. Tanaka, "Organic-inorganic interaction and the growth mechanism of hydroxyapatite crystals in gelatin matrices between 37 and 80 degrees C," *Journal of Materials Science*, vol. 17, no. 4, pp. 387–396, 2006.

[80] O. C. Wilson Jr. and J. R. Hull, "Surface modification of nanophase hydroxyapatite with chitosan," *Materials Science and Engineering: C*, vol. 28, no. 3, pp. 434–437, 2008.

[81] K. Ganguly, T. M. Aminabhavi, and A. R. Kulkarni, "Colon targeting of 5-fluorouracil using polyethylene glycol cross-linked chitosan microspheres enteric coated with cellulose acetate phthalate," *Industrial & Engineering Chemistry Research*, vol. 50, no. 21, pp. 11797–11807, 2011.

[82] R. S. T. Aydın and M. Pulat, "5-Fluorouracil encapsulated chitosan nanoparticles for pH-stimulated drug delivery: evaluation of controlled release kinetics," *Journal of Nanomaterials*, vol. 2012, Article ID 313961, 10 pages, 2012.

[83] J. Mihaly, S. Sterkel, H. M. Ortner et al., "FTIR and FT-Raman spectroscopic study on polymer based high pressure digestion vessels," *Croatica Chemica Acta*, vol. 79, no. 3, pp. 497–501, 2006.

[84] T. Scharnweber, C. Santos, R. P. Franke, M. M. Almeida, and M. E. V. Costa, "Influence of spray-dried hydroxyapatite-5-fluorouracil granules on cell lines derived from tissues of mesenchymal origin," *Molecules*, vol. 13, no. 11, pp. 2729–2739, 2008.

[85] W. Sukaraseranee, S. Watcharamaisakul, B. Golman, and J. Suwanprateeb, "Effect of process parameters on characteristics of spray-dried hydroxyapatite granules," *Key Engineering Materials*, vol. 728, pp. 341–346, 2016.

[86] C. Chen, Z. Huang, W. Yuan, J. Li, X. Cheng, and R.-a. Chi, "Pressure effecting on morphology of hydroxyapatite crystals in homogeneous system," *CrystEngComm*, vol. 13, no. 5, pp. 1632–1637, 2010.

[87] J. Fan, H. Zhang, M. Yi, F. Liu, and Z. Wang, "Temperature induced phase transformation and in vitro release kinetic study of dihydromyricetin-encapsulated lyotropic liquid crystal," *Journal of Molecular Liquids*, vol. 274, pp. 690–698, 2019.

[88] R. B. Diasio and B. E. Harris, "Clinical pharmacology of 5-fluorouracil," *Clinical Pharmacokinetics*, vol. 16, no. 4, pp. 215–237, 1989.

[89] N. Tan, K. Ji, D. He et al., "Research on a kind of biocompatible molecularly imprinted materials with silybin controlled release based on pH/temperature dual responses," *Reactive and Functional Polymers*, vol. 147, article 104449, 2020.

[90] J. A. Ferreira, P. de Oliveira, and E. Silveira, "Drug release enhanced by temperature: an accurate discrete model for solutions in H^3," *Computers & Mathematics with Applications*, vol. 79, no. 3, pp. 852–875, 2020.

[91] E. Kahraman, *Research on drug release performance of hydroxyapatite-gelatin composites produced in SBF medium*, Master Thesis, Istanbul Technical University, Istanbul, 2016.

[92] B. Singh, K. Sharma, Rajneesh, and S. Dutt, "Dietary fiber tragacanth gum based hydrogels for use in drug delivery applications," *Bioactive Carbohydrates and Dietary Fibre*, vol. 21, p. 100208, 2020.

[93] Z. Zhou, S. He, T. Huang et al., "Preparation of gelatin/-hyaluronic acid microspheres with different morphologies for drug delivery," *Polymer Bulletin*, vol. 72, no. 4, pp. 713–723, 2015.

[94] J. L. Arias, "Novel strategies to improve the anticancer action of 5-fluorouracil by using drug delivery systems," *Molecules*, vol. 13, no. 10, pp. 2340–2369, 2008.

[95] S. R. Khan, M. Tawakkul, V. A. Sayedd, P. Faustino, and M. A. Khan, "Stability characterization, kinetics and mechanism of degradation of dantrolene in aqueous solution: effect of pH and temperature," *Pharmacology & Pharmacy*, vol. 3, no. 3, pp. 281–290, 2012.

[96] M. H. Shoaib, J. Tazeen, H. A. Mierchant, and R. I. Yousuf, "Evaluation of drug release kinetics from ibuprofen matrix tablets using HPMC," *Pakistan Journal of Pharmaceutical Sciences*, vol. 19, no. 2, pp. 119–124, 2006.

[97] G. O. Elhassan, "Design and evaluation of controlled release matrix tablet of aspirin by using hydrophobic polymer," *International Journal of Pharmaceutical Research & Allied Sciences*, vol. 6, no. 4, pp. 32–41, 2017.